

# Fracture strength of low-pressure injection-moulded reaction-bonded silicon nitride

S. J. KWAK\*

*The Institute of Materials Processing, Michigan Technological University, Houghton, Michigan 49931, USA*

E. KRUG, S. C. DANFORTH

*Center for Ceramic Research, Rutgers University, P.O. Box 909, New Brunswick, NJ 08855-0909, USA*

Reaction-bonded silicon nitride (RBSN) samples were fabricated via a low-pressure injection-moulding technique. Sample batches of 58, 68, and 70 vol % silicon solids loading were moulded using a multicomponent, nonaqueous binder. These samples were analysed in terms of their nitrified bulk density, flexural strength, and microstructure. Bulk densities of  $2.9 \text{ g cm}^{-3}$  (91% theoretical density) and three-point moduli of rupture in excess of 304 MPa ( $44 \times 10^3 \text{ p.s.i.}$ ) were achieved. These results indicate a potential use of low-pressure injection moulding as a forming technique for the fabrication of RBSN components.

## 1. Introduction

Several forming techniques have been employed in the fabrication of green silicon compacts used to create reaction-bonded silicon nitride (RBSN) bodies. These techniques include: dry pressing [1], cold isostatic pressing [2], and slip casting [3]. The advancement of ceramic materials into high-temperature, high-strength structural applications which require complex shapes, has led to renewed interest in the injection-moulding process as an alternative forming technique. The injection moulding of ceramic materials, which began in the early 1930s, was first reviewed by Schwartzwalder [4] and most recently by Edirisinghe and Evans [5, 6].

Injection moulding has several advantages over traditional forming techniques. One is its ability to fabricate structures from ceramic materials (non-clay based) which do not exhibit an inherent plasticity. A second is its ability to produce highly complex shapes, such as turbine rotors and blades, with good dimensional tolerances. These near net shape bodies minimize the amount of time-consuming diamond grinding needed, thereby greatly reducing production costs. A third advantage is its potential as an automated, high-volume process. As the growth of ceramic materials into numerous innovative structural applications occurs, the necessity for the advancement of ceramic injection-moulding technology appears imperative.

Injection moulding can be divided into two distinct categories: high-pressure and low-pressure injection moulding [7]. High- and low-pressure injection moulding processes differ primarily in the moulding pressure employed and consequently in the nature and volume fraction of binder required. Low-pressure in-

jection moulding typically employs pressures up to 0.69 MPa (100 p.s.i.), low viscosity binders and binder contents between 25 and 50 vol %. High-pressure injection moulding employs pressures between 6.9 and 140 MPa ( $1\text{--}20 \times 10^3 \text{ p.s.i.}$ ), higher viscosity binders, and binder contents of 15–40 vol % [6]. The transcendent advantages of low-pressure injection moulding are its simplicity and cost. Low-pressure injection moulding employs low moulding temperatures (typically  $< 100^\circ\text{C}$ ), and does not require expensive dies or machinery (such as a plunger or auger). However, low-pressure injection moulding does have limitations on part size, shape complexity, and filler solids loading. In addition, the lower viscosity binders may yield low green strengths and the increased binder content may tend to complicate binder removal.

The focus of this research was: (1) the development of a multicomponent binder system which is suitable for the low-pressure injection moulding of Si powder, (2) the fabrication of RBSN bend bar test samples via low-pressure injection moulding, and (3) an evaluation of the nitrified bulk density, flexural strength, and microstructure of these samples as a function of Si solids loading.

## 2. Experimental procedure

A multicomponent binder system was developed through an analysis of the thermal degradation behaviour of several individual components. This analysis was accomplished through the use of a thermogravimetric analyser (TGA). The nonaqueous binder system consisted of a major binder component, a minor binder component and a surfactant. Paraffin wax was

\* Present address: Diamonite Products, W.R. Grace and Co.—Coun. Shreve, OH 44676.

TABLE I Characteristics of RBSN sample batches

Sample batch	Solids loading (%)/density ( $\text{g cm}^{-3}$ )			% Nitridation	
	Initial	Post-BBO	Post-N <sub>2</sub>	Weight gain	XRD
A	58/1.74	68/1.60	81/2.59	93.3	98.4
B	68/1.89	75/1.76	90/2.87	89.6	98.7
C	70/1.93	76/1.79	92/2.93	88.9	98.4

chosen as the major binder component based upon its low viscosity, its ability to be removed at a realistic rate, and its low residual carbon content. The minor binder component employed was stearic acid to act as a lubricant. A Si-based organometallic surfactant ( $\text{C}_{18}\text{H}_{37}\text{Si}(\text{OCH}_3)_3$ ) was used to promote wetting and dispersion [8]. The fabrication of samples was accomplished via the low-pressure injection moulding of commercial grade Si powder (99% + purity). Three sample batches were prepared (Table I). Compounding was performed in the double planetary mixer. Batches ( $400 \text{ cm}^3$ ) were mixed at  $70^\circ\text{C}$  for 12 h. This allowed for substantial powder de-agglomeration as evinced by the mixtures' increased fluidity. Moulding was performed between  $60$  and  $70^\circ\text{C}$ , using an injection pressure of  $0.48$ – $0.55 \text{ MPa}$  ( $70$ – $80 \text{ p.s.i.}$ ), and injection hold times ranging from  $10$ – $15 \text{ s}$ .

Binder removal was performed in a sealed alumina tube furnace. Samples were placed in a high-purity alumina refractory boat and embedded in fine  $\text{Si}_3\text{N}_4$  powder. Extra dry nitrogen (99.98% purity) flowed through the tube at a flow rate of  $85 \text{ l h}^{-1}$ , while a partial vacuum was applied. The heating schedule involved heating to  $600^\circ\text{C}$  at a rate of  $60^\circ\text{C h}^{-1}$ , followed by a 2 h soak at  $600^\circ\text{C}$ , and cooling at a rate of  $300^\circ\text{C h}^{-1}$ . Complete binder removal time totalled less than 15 h. Thermogravimetric analysis was subsequently employed to confirm that binder removal was complete.

Nitridation was performed in a cold-walled furnace with a nitrogen demand cycle. The atmosphere consisted of ultra-high-purity nitrogen ( $< 10 \text{ p.p.m.}$  impurities). Samples were placed in a cylindrical high-purity alumina crucible and the overall sample mass was kept constant at  $14.5$ – $15.0 \text{ g}$ . This is an important parameter to control because it inevitably controls the actual heating rate of the furnace. After evacuation to  $7 \times 10^{-4} \text{ Pa}$ , the samples were heated to  $1000^\circ\text{C}$  at a rate of  $1000^\circ\text{C h}^{-1}$  and held for 0.5 h. Nitrogen was then bled into the system until the  $\text{N}_2$  pressure in the furnace chamber was  $34.5 \text{ kPa}$  ( $5 \text{ p.s.i.g.}$ ). The programmed heating rate was  $60^\circ\text{C h}^{-1}$  from  $1000$ – $1390^\circ\text{C}$ , at which point the samples were held for 6 h. This  $\text{N}_2$  demand cycle [9] resulted in an actual heating rate of approximately  $15^\circ\text{C h}^{-1}$  between  $1100$  and  $1390^\circ\text{C}$  and a total nitridation time of less than 35 h.

Bulk densities were determined through a measurement of each individual bar's dimensions and weight. Modulus of rupture (MOR) measurements were made using a three-point bend configuration, with a cross-head speed of  $0.005 \text{ cm min}^{-1}$  and a span of  $3.18 \text{ cm}$ .

### 3. Results and discussion

The Si powder had a density of  $2.35 \text{ g cm}^{-3}$  ( $\rho_{\text{theoretical}} = 2.33 \text{ g cm}^{-3}$ ), an average particle size of  $5 \mu\text{m}$ , and a surface area of  $1.29 \text{ m}^2 \text{ g}^{-1}$ .

The rheological behaviour of the three injection moulding batches was investigated. The shear rate range investigated was up to and including  $100 \text{ s}^{-1}$ . Batch A, which contained the lowest Si content, exhibited the lowest viscosity of  $2171 \text{ mPa s}$  at  $100 \text{ s}^{-1}$ . Batch B, which contained 10 vol % more Si than that in A, exhibited a viscosity which was four times greater than A ( $9327 \text{ mPa s}$  at  $100 \text{ s}^{-1}$ ). The viscosity of Batch C was significantly greater than that of B despite containing only 2.5 vol % Si more than B (Fig. 1). Owing to this viscosity increase the apparent viscosity of Batch C could not be determined at  $100 \text{ s}^{-1}$ . All three batches exhibited shear thinning behaviour.

Thermogravimetric analysis of the three phase binder system was conducted under conditions which mimicked those employed during the actual binder removal process (Fig. 2). The degradation of the binder began at approximately  $150^\circ\text{C}$  with the majority of the binder, in excess of 90.0%, being removed in the  $150$ – $300^\circ\text{C}$  temperature range. Approximately 1.0% residual binder remained at  $600^\circ\text{C}$ .

The per cent nitridation of the Si compacts was examined using sample weight gain and X-ray diffraction [10], Table I. As expected, the reaction percentage decreased with increased solids loading due to the

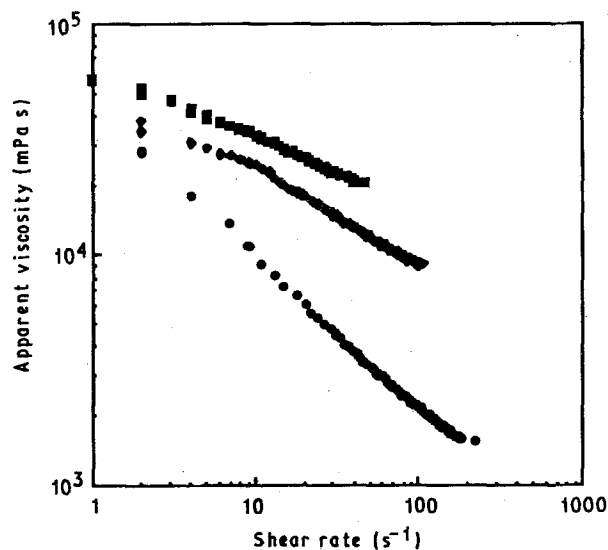


Figure 1 Apparent capillary viscosity as a function of shear rate. Batch (●) A, (◆) B, (■) C.

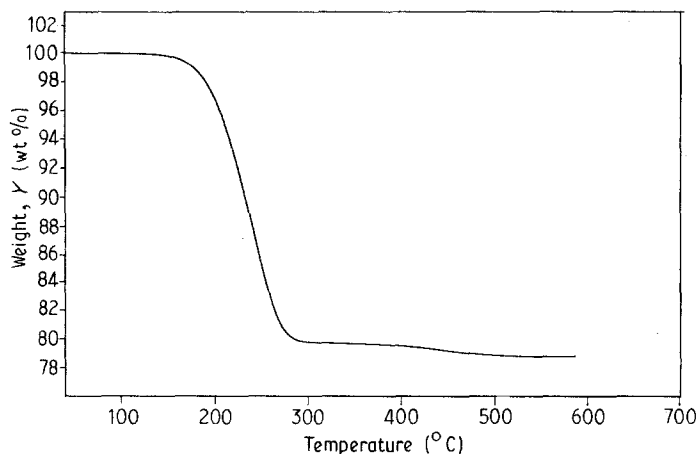


Figure 2 Thermogravimetric analysis ( $N_2$  gas at  $1^\circ C \text{ min}^{-1}$ ) of binder system used in low-pressure injection-moulded Si sample (Batch A).  $T_1 = 49.193^\circ C$ ,  $T_2 = 586.490^\circ C$ ,  $Y_1 = 99.996 \text{ wt } \%$ ,  $Y_2 = 78.774 \text{ wt } \%$ ,  $\Delta Y = -21.222 \text{ wt } \%$ .

increased green densities of the Si compacts. While higher green densities have been found to produce superior strengths, a decrease in  $N_2$  accessibility to the inner regions of the Si compact has been observed, which tends to halt the reaction prior to completion [11]. Batches A, B and C were found to have  $\alpha/\beta$  phase ratios of 1.6, 1.8, and 1.1, respectively. The literature [1] indicates that a high  $\alpha/\beta$  ratio generally results in reduced flaw size and an improved microstructure, which in turn tends to result in RBSN components which exhibit superior mechanical properties. Therefore, X-ray diffraction analysis has revealed that while the Si compacts were nitrified to near completion, the amount of the desirable  $\alpha\text{-Si}_3\text{N}_4$  present is relatively low.

As expected, there was a positive relationship between initial Si solids loading and final nitrified density (Fig. 3). The mean bulk densities (Table I) were found to be 2.59, 2.87, and  $2.93 \text{ g cm}^{-3}$ , or 81%, 90% and 92% theoretical density for Batches A, B, and C, respectively. These values are considerably greater than expected, as theoretically, the maximum attainable bulk densities are 2.27, 2.65 and  $2.73 \text{ g cm}^{-3}$  for RBSN components with 58, 68 and 70 vol % solids loading, respectively. The elevated bulk density values were due to a 6–10 vol % shrinkage which occurred during binder removal. Therefore, the injection-moulded samples with initial solids loadings of 58, 68 and 70 vol % resulted in Si compacts (post-binder removal) and subsequently RBSN samples of much greater densities.

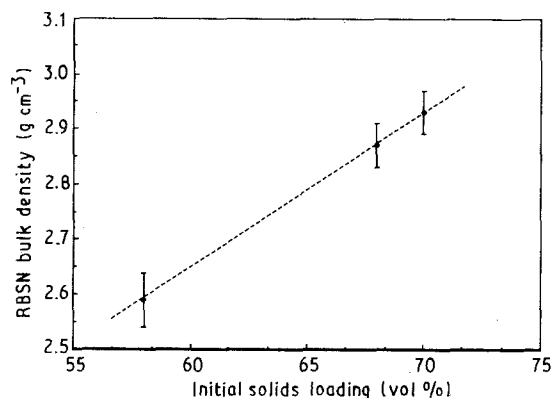


Figure 3 Dependence of RBSN bulk density on initial Si solids loading.

The possibility that impurities contributed to the bulk densities was also investigated. Through elemental analysis by EDX, it was determined that the single significant impurity present was Fe. All three sample batches contained less than 0.4 wt % Fe, which is comparable to that present in the original Si powder. This analysis indicates that the experimental bulk density values are not the result of a significant heavy element impurity content.

The mean modulus of rupture (three-point) values for Batches A, B and C were found to be 204 MPa ( $29.5 \times 10^3 \text{ p.s.i.}$ ), 291 MPa ( $42.2 \times 10^3 \text{ p.s.i.}$ ) and 305 MPa ( $44.2 \times 10^3 \text{ p.s.i.}$ ). Fig. 4 demonstrates the expected positive dependence of flexural strength upon Si solids loading. The mechanical property results compare quite favourably with that available in the literature. Washburn and Baumgartner [12] reported a mean MOR (three-point) value of 296 MPa with a standard deviation of 52.4 MPa for NC-350 samples. Danforth and Richman [13] have previously presented mean MOR (four-point) values as high as 290 MPa. Utilizing a  $N_2$  demand cycle similar to that used in this analysis, Mangels [9] reported mean MOR (four-point) results of 207 MPa and a standard deviation of 35 MPa.

Optical micrographs (Fig. 5a, b) indicate that all three sample microstructures exhibited a low  $\alpha/\beta$  phase ratio, in agreement with X-ray diffraction. Large  $\beta\text{-Si}_3\text{N}_4$  grains were evident as well as a fine  $\alpha\text{-Si}_3\text{N}_4$  matte phase. It is this  $\alpha\text{-Si}_3\text{N}_4$  matte phase which possesses the microstructure generally considered

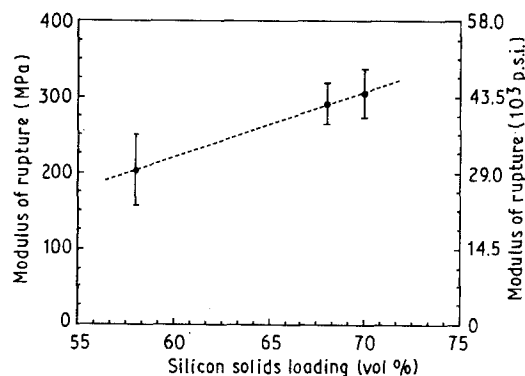


Figure 4 Effect of initial Si solids loading on flexural strength (three-point bend) of RBSN. Each data point is an average of ten samples.

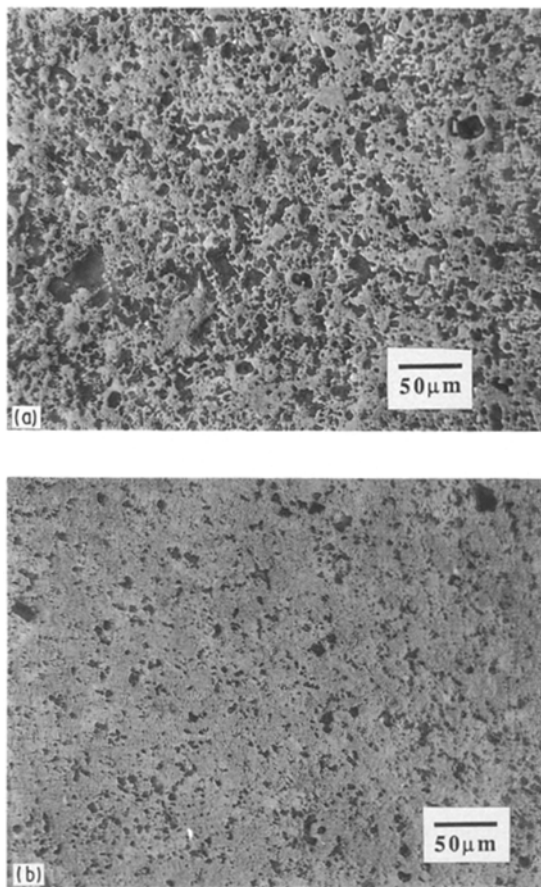


Figure 5 Optical micrographs of low- and high-density RBSN: (a) 58 vol % Si sample (Batch A); (b) 70 vol % Si sample (Batch C).

desirable in RBSN components. Batch A samples were more porous and showed a wider pore size distribution (ranging from approximately  $< 1 \mu\text{m}$  to nearly  $100 \mu\text{m}$  diameter), than Batch B or C. These samples were found to consist largely of interconnected, irregularly shaped pores. The amount of residual Si present appeared to be very low and well dispersed. Batch C samples exhibited a significantly narrower pore size distribution, ranging from approximately  $< 1 \mu\text{m}$  to  $50 \mu\text{m}$ , with the majority in the  $10\text{--}20 \mu\text{m}$  range. The amount of residual Si present was slightly greater and not as well dispersed, as that in batch A samples.

Several key processing parameters, not specifically addressed in this analysis, have also been shown to enhance significantly the mechanical properties of RBSN [9, 14–17]. These processing parameters include: (1) the Si powder size, distribution, and purity, (2) the nitridation cycle (which controls the  $\alpha/\beta$  ratio), (3) the nitridation atmosphere, and (4) the final surface finish. It is therefore hypothesized that an optimization of these key variables may provide for substantial increases in the mechanical properties of low-pressure injection-moulded RBSN.

#### 4. Conclusion

A multicomponent, nonaqueous binder system was developed for the low-pressure injection moulding of Si. This binder consisted of paraffin wax, stearic acid and an Si-based organometallic dispersant. This formulation was chosen based upon its workable vis-

cosity and its ability to be removed at a realistic rate. Sample batches of 58, 68, and 70 vol % Si solids loading (Batches A, B and C) were low-pressure injection moulded. After binder removal, these Si compacts were successfully nitrided to near completion with  $\alpha/\beta$  ratios ranging from 1.1–1.8. These RBSN samples exhibited a maximum bulk density of  $> 90\%$  theoretical despite an Fe content of less than 0.40 wt %. Flexural strengths (three-point MOR) were 204 MPa ( $29.5 \times 10^3$  p.s.i.), 291 MPa ( $42.2 \times 10^3$  p.s.i.), and 305 MPa ( $44.2 \times 10^3$  p.s.i.) for Batches A, B and C, respectively. Optical micrographs revealed that the higher density RBSN possessed a desirable microstructure. These results indicate that the potential exists for the use of low-pressure injection moulding as a technique for fabricating RBSN components with desirable properties.

#### Acknowledgements

The authors thank the National Science Foundation, University of Delaware, Rutgers University Center for Composites Manufacturing Science and Engineering, and the New Jersey Commission on Science and Technology for their support of this work, and also Dr R. Anderson, P. Beke, and Dr I. Tsao for their assistance and suggestions.

#### References

1. A. G. EVANS and R. W. DAVIDGE, *J. Mater. Sci.* **5** (1970) 314.
2. B. F. JONES and M. W. LINDLEY, *ibid.* **10** (1975) 967.
3. A. EZIS, in "Ceramics for High Performance Applications", edited by J. J. Burke, A. E. Gorum and R. N. Katz (Brook Hill, Chestnut Hill, MA, 1974) p. 207.
4. K. SCHWARTZWALDER, *Amer. Ceram. Soc. Bull.* **28** (1949) 459.
5. M. J. EDIRISINGE and J. R. G. EVANS, *Int. J. High Technol. Ceram.* **2** (1986) 1.
6. *Idem*, *ibid.* **2** (1986) 249.
7. A. F. HENRIKSEN, "Injection-Molded and Sintered Metal, Ceramic and Cermet Parts", presented at the Gorham Conference, San Diego, CA, 1–3 February 1987.
8. G. KRUG and S. C. DANFORTH, "Proceedings of the Third International Symposium on Ceramic Materials and Components for Engines", Las Vegas, Nevada, November 1988, edited by V. J. Tennery (American Ceramic Society, Westerville, OH 1989) p. 237.
9. J. A. MANGELS, *J. Amer. Ceram. Soc.* **58** (1981) 613.
10. C. P. GAZZARA and D. R. MERSEIER, *Amer. Ceram. Soc. Bull.* **56** (1977) 777.
11. J. A. MANGELS and R. M. WILLIAMS, *ibid.* **62** (1983) 601.
12. M. E. WASHBURN and H. R. BAUMGARTNER, in "Ceramics For High Performance Applications II", edited by J. J. Burke, A. E. Gorum and R. N. Katz, (Brook Hill, Chestnut Hill, MA, 1974) p. 479.
13. S. C. DANFORTH and M. H. RICHMAN, *Amer. Ceram. Soc. Bull.* **62** (1983) 501.
14. A. J. MOULSON, *J. Mater. Sci.* **14** (1979) 1017.
15. S. C. DANFORTH, PhD Thesis, Brown University, June 1978.
16. M. W. LINDLEY, D. P. ELIAS, B. F. JONES and K. C. PITMAN, *J. Mater. Sci.* **14** (1979) 70.
17. J. S. HAGGERTY, G. J. GARVEY, J. H. FLINT, B. W. SHELDON, M. AOKI and M. OKUYAMA, *Ceram. Trans.* **1** (1988) 1059.

Received 19 February

and accepted 19 November 1990